Effect of scattering lengths on the dynamics of a two-component Bose-Einstein condensate

Gábor Csire,[1,2,*] Dániel Schumayer,[3,†] and Barnabás Apagyi[1,‡]
[1]Institute of Physics, Budapest University of Technology and Economics, Budafoki út 8, Budapest H-1111, Hungary
[2]Institute of Physics, Eötvös Loránd University, Pázmány Péter sétány 1/A, Budapest H-1117, Hungary
[3]Jack Dodd Centre for Quantum Technology, Department of Physics, University of Otago, 730 Cumberland St., Dunedin 9016, New Zealand
(Received 9 September 2010; published 7 December 2010)

We examine the effect of the intra- and interspecies scattering lengths on the dynamics of a two-component Bose-Einstein condensate, particularly focusing on the existence and stability of solitonic excitations. For each type of possible soliton pairs, stability ranges are presented in tabulated form. We also compare the numerically established stability of bright-bright, bright-dark, and dark-dark solitons with our analytical prediction and with that of Painlevé analysis of the dynamical equation. We demonstrate that tuning the interspecies scattering length away from the predicted value (keeping the intraspecies coupling fixed) breaks the stability of the soliton pairs.

DOI: 10.1103/PhysRevA.82.063608 PACS number(s): 03.75.Kk, 03.75.Mn

I. INTRODUCTION

Since Bose-Einstein condensates (BECs) can be routinely prepared in laboratories, ultracold gases became a very important test bed for many predictions of condensed-matter physics [1]. The experimental examination of binary condensates started nearly the same time as for single condensates by using two different quantum states of the same species, such as ^{87}Rb [2] or ^{23}Na [3]. With the development of sympathetic cooling, ultracold mixtures have been assembled from two different alkalies (^{41}K–^{87}Rb [4,5], ^{7}Li–^{133}Cs [6], and ^{87}Rb–^{133}Cs [7]) or for different isotopes of the same alkali atom (^{85}Rb–^{87}Rb [8]). The tunability of the inter- and intraspecies scattering lengths via driving the mixture through a Feshbach resonance has also been experimentally demonstrated [5,7].

The ability to create Bose-Einstein condensate(s), a highly coherent form of matter, also facilitated the convergence of two fields of physics—condensed matter physics and quantum optics—and therefore BECs became favorable candidates for examining the effects of nonlinearity in matter waves, where this nonlinearity originates from the mean-field representation of the interatomic interaction. The similarity between electromagnetic waves in a nonlinear medium and coherent matter waves is also expressed in the equations of motion—the nonlinear Schrödinger equation (NLS) for the former and the Gross-Pitaevskii (GP) equation for the latter. Although the physical interpretations of these equations are different, their structures are the same, apart from the external potential term. Furthermore, in some cases this extra term can even be removed [9] and the GP equation is transformed into a form coinciding with the NLS equation. Consequently, all results for the NLS equation known in nonlinear optics can be readily adapted to Bose-Einstein condensates.

One of the surprising phenomena of nonlinear optics is the existence of particle-like waveforms, the so-called solitons [10]. Such excitations have already been experimentally observed in single- or two-component Bose-Einstein condensates: dark solitons [11,12], bright solitons [13,14], their two-component coupled analogs, the dark-dark [15], bright-bright [16], or even dark-bright [17,18] multicomponent solitary waves [18,19].

However, the question of the existence of solitons needs more attention than simply recognizing the similarity between the two governing equations. The existence of solitons is strongly related to the integrability of the given physical model. A usual test to determine whether or not an equation is integrable is the Painlevé test (P test) [20]. It was shown that without any potential term or inhomogeneity the one-dimensional NLS equation, $iu_t + u_{xx} \pm 2|u|^2 u = 0$, is completely integrable both in its one-component [20,21] or multicomponent [22,23] form. However, the inclusion of a potential term, $v(x,t)u$, in the one-component NLS equation or different coupling strengths in the multicomponent NLS or GP equations fundamentally changes their integrability [24,25]. It has been shown that integrability is preserved provided the external potential, $v(x,t)$, has a specific form [25]. Schumayer and Apagyi [26] examined the integrability of the two-component coupled Gross-Pitaevskii (CGP) equations and reached a similar conclusion: The scattering lengths and the external potentials cannot be arbitrary if the integrability of CGP is to be preserved. The inter- and intraspecies scattering lengths must satisfy the following equation:

$$\frac{2\xi_1\xi_2 - \kappa_1\xi_1 - \kappa_2\xi_2}{\xi_1\xi_2 - \kappa_1\kappa_2} = \frac{(2n+1)^2 + 7}{16}, \qquad (1)$$

where $\xi_1 = a_{11}/a_{21}$, $\xi_2 = a_{22}/a_{12}$, $\kappa_1 = \mu_{11}/\mu_{21}$, $\kappa_2 = \mu_{22}/\mu_{12}$, and μ_{ij} denotes the reduced mass of a pair of particles composed of an atom from the ith and jth species. On the right-hand side of Eq. (1), n is a non-negative integer. One may call n a *classification number*, because it determines the form of the external potentials for which CGP equations remain integrable. For example, for $n = 2$, the external potential, apart from the quadratic trapping potential, may even contain an imaginary time-dependent term [26]. This term can mimic the loss or gain in the number of particles of the given species. We note here that usually dissipation works against long-living coherent matter waves; however, the importance of this imaginary potential term has been analyzed in Refs. [27,28] and shown to permit exact soliton solution [29]. In the context of BECs at finite temperature,

*csire.gabor@wigner.bme.hu
†dschumayer@physics.otago.ac.nz
‡apagyi@phy.bme.hu

the interaction of the condensate with the thermal cloud could also be taken into account as an imaginary term in the governing GP equation. This interaction, due to its stochastic nature, can influence the dynamics of the solitons, via density fluctuation.

In this paper we carry out an analysis on how the intra- and interspecies interactions influence the dynamics of a binary mixture of Bose-Einstein condensates. We select out of the many possible systems of two-component BECs the pairs ^{87}Rb–^{87}Rb (prepared in two distinct hyperfine states), ^{23}Na–^{87}Rb, and ^{7}Li–^{39}K. In the former two systems it is possible to study the stability of bright-dark and dark-dark soliton pairs, while the last pair is capable of sustaining bright-bright and bright-dark excitations.

The organization of the paper is as follows: Section II defines a quasi-one-dimensional model derived from the general three-dimensional, coupled Gross-Pitaevskii equations, assuming a cigar-like harmonic oscillator trap potential. In the first part of Sec. III we perform a stability analysis based on coupled soliton excitations and on Eq. (1) of the P test. In the second part of Sec. III, possible new interesting modes exhibited by the bright-bright solitons will be shown. Section IV is devoted to a conclusion and the summary.

II. THE MODEL

In ultracold gases the interaction between two particles can usually be well described by a scalar parameter, the scattering length. For a two-component Bose-Einstein condensate one has to introduce three, possibly different, scattering lengths, characterizing the intraspecies interactions (a_{11}, a_{22}) and the interspecies coupling ($a_{12} = a_{21}$).

In the mean-field approximation a two-component BEC is described by the coupled Gross-Pitaevskii equations [30,31] in the form

$$i\hbar \frac{\partial}{\partial t}\Psi_i = \left[-\frac{\hbar^2}{2m_i}\Delta + \sum_{j=1}^{2}\Omega_{ij}|\Psi_j|^2 + V_i \right]\Psi_i, \qquad (2)$$

where m_i denotes the individual mass of the ith atomic species, $\Omega_{ij} = 2\pi\hbar^2 a_{ij}/\mu_{ij}$ with a_{ij} being the three-dimensional scattering length, $\mu_{ij} = m_i m_j/(m_i + m_j)$ is the reduced mass, and V_i denotes the external trapping potential. In the following, indices i and j label the components, and therefore they take only two values, 1 and 2. In the case of real trap potentials the normalization of the wave functions reads as $N_i = \int |\Psi_i|^2 dV$, with N_i denoting the number of atoms in the ith component. We exclude those cases from our analysis where the species can transform into each other; therefore, the number of atoms in each component hereafter is conserved.

A. Transformed equations

If the three-dimensional quadratic trapping potential is weak in one direction, i.e.,

$$V_i = \tfrac{1}{2}m_i\left[\omega_{i,x}^2 x^2 + \omega_{i,\perp}^2 (y^2 + z^2)\right], \qquad (3)$$

where $\omega_{i,x} \ll \omega_{i,\perp}$, one may replace the three-dimensional equations Eq. (2) with a coupled system of quasi-one-dimensional GP equations. Although Eq. (2) is a nonlinear equation, physically we may assume that the weak x direction decouples from the strong yz plane; therefore, the macroscopic wave functions can be written as

$$\Psi_i(\mathbf{r},t) = \sqrt{N_1}\,\psi_i(x,t)\,\chi_{i,\perp}(y,z,t), \qquad (4)$$

where $\chi_{i,\perp}$ represents the ground-state solution of the corresponding two-dimensional Schrödinger equation in the yz plane. The external potential introduces suitable units of length and time as $a_\perp = \sqrt{\hbar/m_1\omega_{1,\perp}}$ and $\tau = 1/\omega_{1,\perp}$, respectively. By rescaling the spatial and temporal variable with $a_\perp$ and τ one obtains two quasi-one-dimensional GP equations:

$$i\psi_{1,t} = \left[-\frac{1}{2}\partial_{xx} + \frac{\lambda_1^2}{2}x^2 + b_{11}|\psi_1|^2 + b_{12}|\psi_2|^2 \right]\psi_1, \qquad (5a)$$

$$i\psi_{2,t} = \left[-\frac{\kappa}{2}\partial_{xx} + \frac{\lambda_2^2}{2\kappa}x^2 + b_{21}|\psi_1|^2 + b_{22}|\psi_2|^2 \right]\psi_2, \qquad (5b)$$

where $b_{11} = 2a_{11}N_1$, $b_{22} = 2a_{22}N_1\kappa/\gamma$, $b_{12} = b_{21} = 2a_{12}N_1(1+\kappa)/(1+\gamma)$, $\gamma = \omega_{2,\perp}/\omega_{1,\perp}$, $\kappa = m_1/m_2$, $\lambda_1 = \omega_{1,x}/\omega_{1,\perp}$, and $\lambda_2 = \omega_{2,x}/\omega_{1,\perp}$. The normalization is such that $\int|\psi_1|^2 dx = 1$ and $\int|\psi_2|^2 dx = N_2/N_1$. Moreover, the relation $\gamma^2 = \kappa$ must hold if both species experience the same harmonic potential. (Note the slight departure from Ref. [32] in the definition of b_{22}, which, however, may result in a large difference of the values of b_{22} if a two-component condensate contains species with different masses $m_1 \neq m_2$.)

B. Thomas-Fermi background

If the kinetic-energy term is negligible compared to the potential-energy terms in Eqs. (5a) and (5b), then one may apply the Thomas-Fermi approximation to determine the density distribution of the ground state. Following Ref. [33] we write the corresponding wave-functions as

$$\psi_i(x,t) \approx \Phi_i^{\mathrm{TF}}(x)\exp\left(-iE_i^{\mathrm{TF}}t/\hbar\right), \qquad (6)$$

resulting in TF densities

$$\left|\Phi_i^{\mathrm{TF}}\right|^2 = \frac{A_i}{\Delta}\left(x_i^2 - x^2\right) \quad (|x| < x_i) \qquad (7)$$

and TF energies

$$E_1^{\mathrm{TF}} = \left(b_{11}A_1x_1^2 + b_{12}A_2x_2^2\right)/\Delta, \qquad (8a)$$

$$E_2^{\mathrm{TF}} = \left(b_{12}A_1x_1^2 + b_{22}A_2x_2^2\right)/\Delta, \qquad (8b)$$

where $\Delta = b_{11}b_{22} - b_{12}^2$. The parameters A_i and x_i represent the amplitude of the density and the extension of the condensates, respectively. All these quantities are determined by the system parameters b_{ij}, N_i, and λ_i according to the following relations:

$$A_1 = \frac{b_{22}}{2}\lambda_1^2 - \frac{b_{12}}{2\kappa}\lambda_2^2, \quad \text{and} \quad A_2 = \frac{b_{11}}{2\kappa}\lambda_2^2 - \frac{b_{12}}{2}\lambda_1^2, \qquad (9)$$

while the extensions are

$$x_1 = \left(\frac{3}{4}\frac{\Delta}{A_1}\right)^{1/3} \quad \text{and} \quad x_2 = \left(\frac{3}{4}\frac{\Delta}{A_2}\frac{N_2}{N_1}\right)^{1/3}. \qquad (10)$$

Although the Thomas-Fermi density distribution is not physical at $x = x_i$, it still provides a good starting point for analytical calculations. In our numerical treatment we will not use this approximation; instead we start our simulations from the appropriate ground-state solution of the one-dimensional GP equation.

C. Coupled soliton excitations

Now we are seeking solutions of Eqs. (5a) and (5b) that support soliton excitations. A static soliton excitation can be written as [33]

$$\widetilde{\psi}_i(x,t) = \Phi_i^{\mathrm{TF}}(0)\varphi_i(x)\exp(-i\widetilde{E}_i t). \tag{11}$$

By inserting this ansatz into the GP equations (5a) and (5b) and neglecting the small potential contributions one obtains the coupled soliton equations as follows:

$$\widetilde{E}_1\varphi_1 = \left[-\tfrac{1}{2}\,\partial_{xx} + \widetilde{b}_{11}|\varphi_1|^2 + \widetilde{b}_{12}|\varphi_2|^2\right]\varphi_1, \tag{12a}$$

$$\widetilde{E}_2\varphi_2 = \left[-\frac{\kappa}{2}\,\partial_{xx} + \widetilde{b}_{21}|\varphi_1|^2 + \widetilde{b}_{22}|\varphi_2|^2\right]\varphi_2, \tag{12b}$$

with $\widetilde{b}_{ij} = b_{ij}A_j x_j^2/\Delta$. The normalization of the soliton solutions reads as follows:

$$\int_{-L_1}^{L_1} |\varphi_1|^2 dx = \frac{\Delta}{A_1 x_1^2}, \tag{13a}$$

$$\int_{-L_2}^{L_2} |\varphi_2|^2 dx = \frac{\Delta}{A_2 x_2^2}\frac{N_2}{N_1}, \tag{13b}$$

where the integrations, in both cases, are over the spatial extension, L_i, of the solitons.

These coupled equations admit generic moving soliton solutions of the types bright-bright (BB), bright-dark (BD), dark-bright (DB), and dark-dark (DD). We shall investigate here a simple static bright-dark soliton pair solution by taking the first component to be a static bright soliton,

$$\varphi_1^{\mathrm{BD}}(x) = q_1\mathrm{sech}(k_1 x), \quad \varphi_1^{\mathrm{BD}}(x \to \pm\infty) = 0, \tag{14a}$$

and the second component to be the static dark soliton

$$\varphi_2^{\mathrm{BD}}(x) = q_2\tanh(k_2 x), \quad \varphi_2^{\mathrm{BD}}(x \to \pm\infty) = \pm q_2, \tag{14b}$$

with yet unknown complex amplitudes q_i and wave vector k_i. The latter one is related to the width of the soliton, $k_i \sim 1/L_i$. By inserting Eqs. (14a) and (14b) into Eqs. (12a) and (12b) and equating the coefficients of the constant and x-dependent terms, respectively, one may conclude that the wave vectors of the dark and bright solitons must be equal, $k_1 = k_2 \equiv k$. The amplitudes are expressed by the system parameters as

$$|q_1|^2 = \frac{k^2}{A_1 x_1^2}(\kappa b_{12} - b_{22}), \tag{15a}$$

$$|q_2|^2 = \frac{k^2}{A_2 x_2^2}(\kappa b_{11} - b_{12}). \tag{15b}$$

The energy of these excitations read as

$$\widetilde{E}_1^{\mathrm{BD}} = k^2\left(\frac{\kappa b_{11} - b_{12}}{\Delta}b_{12} - \frac{1}{2}\right), \tag{16a}$$

$$\widetilde{E}_2^{\mathrm{BD}} = k^2\,\frac{\kappa b_{11} - b_{12}}{\Delta}b_{22}. \tag{16b}$$

Suppose now that the width parameter k is a real number. The modulus of the amplitudes of the bright-dark soliton pair superimposed on the Thomas-Fermi background must be real numbers; thus one obtains the following set of conditions for the existence of these bright-dark soliton excitations:

$$C_1 \equiv \frac{\kappa b_{12} - b_{22}}{\Delta} \geqslant 0 \quad \text{and} \quad C_2 \equiv \frac{\kappa b_{11} - b_{12}}{\Delta} \geqslant 0. \tag{17}$$

One may apply the same method to generate static bright-bright or dark-dark soliton excitations. In the bright-bright case one obtains the following solutions:

$$\varphi_1^{\mathrm{BB}}(x) = \frac{k}{\sqrt{A_1}x_1}\sqrt{\kappa b_{12} - b_{22}}\,\mathrm{sech}(kx), \tag{18a}$$

$$\varphi_2^{\mathrm{BB}}(x) = \frac{k}{\sqrt{A_2}x_2}\sqrt{b_{12} - \kappa b_{11}}\,\mathrm{sech}(kx), \tag{18b}$$

with the conditions

$$C_1 \geqslant 0 \quad \text{and} \quad C_2 \leqslant 0, \tag{19}$$

while the energies are $\widetilde{E}_1^{\mathrm{BB}} = \widetilde{E}_2^{\mathrm{BB}}/\kappa = -k^2/2$. The dark-dark coupled soliton solutions read as follows:

$$\varphi_1^{\mathrm{DD}}(x) = \frac{k}{\sqrt{A_1}\,x_1}\sqrt{b_{22} - \kappa b_{12}}\,\tanh(kx), \tag{20a}$$

$$\varphi_2^{\mathrm{DD}}(x) = \frac{k}{\sqrt{A_2}\,x_2}\sqrt{\kappa b_{11} - b_{12}}\,\tanh(kx), \tag{20b}$$

with the conditions

$$C_1 \leqslant 0 \quad \text{and} \quad C_2 \geqslant 0, \tag{21}$$

and energies $\widetilde{E}_1^{\mathrm{DD}} = \widetilde{E}_2^{\mathrm{DD}}/\kappa = k^2$. Our interesting result shows that in the bright-bright and dark-dark cases the energies are uniquely determined by the wave vector and the mass ratio. Note that the existence conditions of Eqs. (17), (19), and (21) are just the same as obtained in Ref. [32] for the existence of moving soliton pairs, while the constraints for static excitations were published in Ref. [33].

III. STABILITY TESTS BY SIMULATION

In this section we numerically investigate the stability of soliton pairs. To solve the time-dependent coupled Gross-Pitaevskii equations (5a) and (5b), a third-order-accurate split-step Fourier transform method is used, as described in Ref. [34] for a single-component condensate. Here we solve the time-independent coupled Gross-Pitaevskii equations for their numerically exact ground states using the imaginary time method [35] combined with the split-step operator technique. Choosing initial distributions is necessary to this method, and the Thomas-Fermi approximate solution proved to be an effective initial guess for this purpose.

The procedure explained in the previous section can be generalized for solitons moving with velocity v. Such a solution is given by

$$\widetilde{\psi}_1^{\mathrm{BD}} = \Phi_1^{\mathrm{TF}}(0)\varphi_1^{\mathrm{BD}}(x - vt)\exp\left(-i\widetilde{E}_1^{\mathrm{BD}}t\right) \times \exp\left\{-i\left[v^2 t\left(\frac{b_{12}C_2}{\kappa^2} - \frac{1}{2}\right) - v(x - vt)\right]\right\}, \tag{22a}$$

$$\widetilde{\psi}_2^{\mathrm{BD}} = \left[i\frac{\sqrt{C_2}}{\kappa}v + \Phi_2^{\mathrm{TF}}(0)\varphi_2^{\mathrm{BD}}(x - vt)\right] \times \exp\left(-i\widetilde{E}_2^{\mathrm{BD}}t\right)\exp\left(-i\,\frac{b_{22}C_2}{\kappa^2}v^2 t\right). \tag{22b}$$

TABLE I. Various domains of inter- and intraatomic interaction strengths b_{ij} permitting the existence of a bright-dark soliton pair.

Case	b_{11}	b_{22}	Constraint on b_{12}		
1	+	−	no bright-dark soliton pair		
2	−	+	$b_{11}\kappa < b_{12} < b_{22}/\kappa$		
3a	−	−	$-\sqrt{b_{11}b_{22}} < b_{12} < b_{11}\kappa$	if	$\kappa^2 b_{11} > b_{22}$
3b			$b_{11}\kappa < b_{12} < -\sqrt{b_{11}b_{22}}$	if	$\kappa^2 b_{11} < b_{22}$
4a	+	+	$\sqrt{b_{11}b_{22}} < b_{12} < b_{22}/\kappa$	if	$\kappa^2 b_{11} < b_{22}$
4b			$b_{22}/\kappa < b_{12} < \sqrt{b_{11}b_{22}}$	if	$\kappa^2 b_{11} > b_{22}$

At $v = 0$ we obtain the static soliton excitation solution given by Eq. (11) in the preceding section.

The existence conditions Eq. (17) prescribe various relations between domains of the inter- and intracoupling strengths b_{ij}, where it is possible to create bright-dark soliton pairs. These domains are listed in Table I. Although the creation of a bright soliton is generally associated with attractive interaction ($b_{ii} < 0$) among the particles, Table I clearly shows that, due to the appropriate other couplings, it may also be possible to create a bright soliton in case of repulsive interaction ($b_{ii} > 0$). Such a situation occurs in case 4a of Table I, which we analyze in the following.

A. Moving bright-dark soliton pairs

Let us now investigate the stability of a bright-dark soliton pair for case 4a of Table I by considering two experimentally accessible two-component BECs. The first is composed of the two hyperfine states of ^{87}Rb atoms, and the second is obtained from ^{23}Na and ^{87}Rb atoms. In both cases the scattering lengths are well known and can be tuned over a broad limit by using the Feshbach resonance method. Our aim here is to explore the sensitivity of the temporal evolution of a soliton pair when the interatomic coupling strength b_{12} is varied around the value prescribed by the ratio Eq. (1) obtained by performing a Painlevé analysis of the coupled GP equations [26]. In this respect we fix the intraatomic strengths b_{ii} to values easily accessible to the experiments and vary the interatomic interaction values b_{12} within a small range allowed by case 4a in Table I. In order to represent a more realistic situation, a small velocity of $v = 0.04$ is given to the solitons, a weak harmonic trapping potential is added along the longitudinal direction, and the solitons are superimposed on the ground-state density distribution. This procedure spatially confines the solitons without affecting their essential stability properties [32].

In Fig. 1, we plot a bright-dark soliton pair composed of two hyperfine states of ^{87}Rb atoms. The top two panels show the case when the interspecies interaction is chosen according to Eq. (1). Both solitons oscillate in the harmonic trap in a stable manner with an angular frequency slightly less than $\omega_x/\sqrt{2}$, which the one-dimensional Thomas-Fermi model predicts for a single dark soliton [36]. The difference is probably caused by the presence of the bright soliton, since the bright component fills the dip of the dark soliton; therefore, the dark soliton has to drag this extra mass as well. This effect has recently been observed [18] with a ^{87}Rb–^{87}Rb condensate, prepared in the $|F = 2, m_F = 0\rangle$ (bright soliton) and $|F = 1, m_F = 0\rangle$ (dark soliton) hyperfine states.

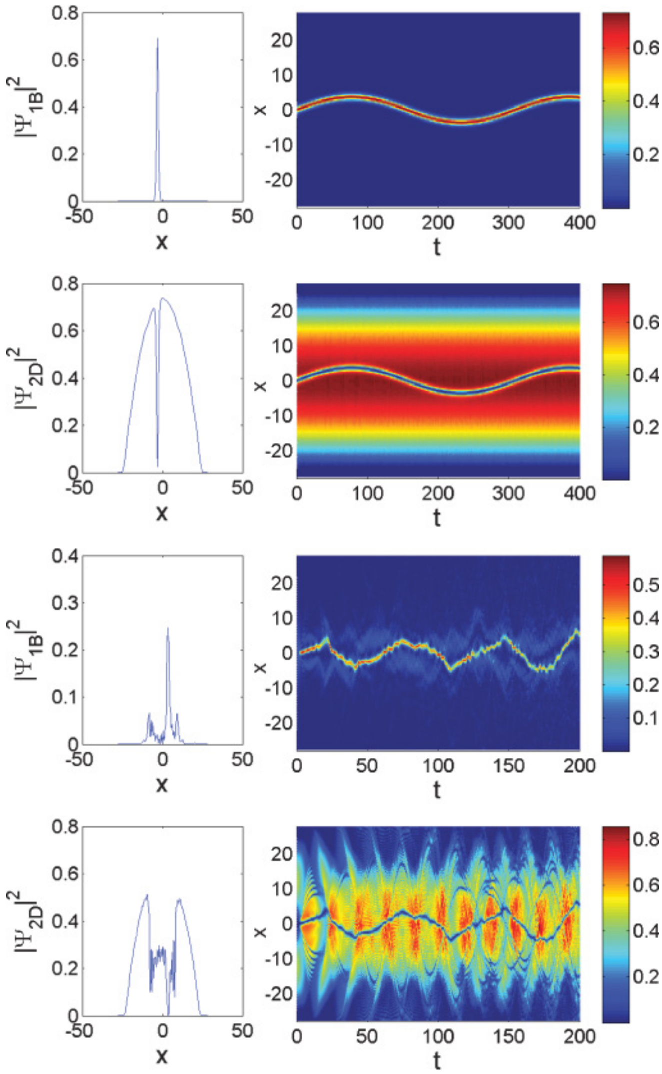

FIG. 1. (Color online) Evolution of the bright-dark solitons of a two-component BEC composed of two hyperfine states of the ^{87}Rb atom, showing the intraspecies scattering length $a_{12} = 5.5$ nm ($b_{12} = 13.6$) satisfying the ratio formula of Eq. (1) (top two panels) and $a_{12} = 5.4$ nm ($b_{12} = 13.35$) disobeying the ratio formula (bottom two panels). Other parameters are $a_{11} = 0.8 \times 5.5$ nm ($b_{11} = 10.88$), $a_{22} = 1.2 \times 5.5$ nm ($b_{22} = 16.32$), $m_1 = m_2 = 87$ a.u., $\omega_{1,\perp} = 2\pi \times 710$ Hz, $\lambda_1 = \lambda_2 = 0.2$, $v = 0.04$, $N_1 = 500$, and $N_2 = 6600$. The snapshots depict the soliton pairs at $t = 200$ and $t = 20$, respectively. The distance x and time t are measured in units of $a_\perp = 404.5$ nm and $\tau = 0.22$ ms.

However, if a_{12} (or equivalently b_{12}) is tuned away from this particular value, the stability is lost, and the initial forms of the solitons are destroyed by the destructive interference of the constantly emitted and recaptured sound waves. It is worthwhile to mention, although only as a qualitative statement, that the appearance of sound waves made the solitons' oscillation faster (see the different range of time in the top two and bottom two panels of Fig. 1). The sound waves travel faster than the solitons, and after being reflected back from the edge of the condensate they collide with the solitons. The subsequent collisions possibly speed up the oscillation and turn it into an irregular sloshing. Despite the irregular

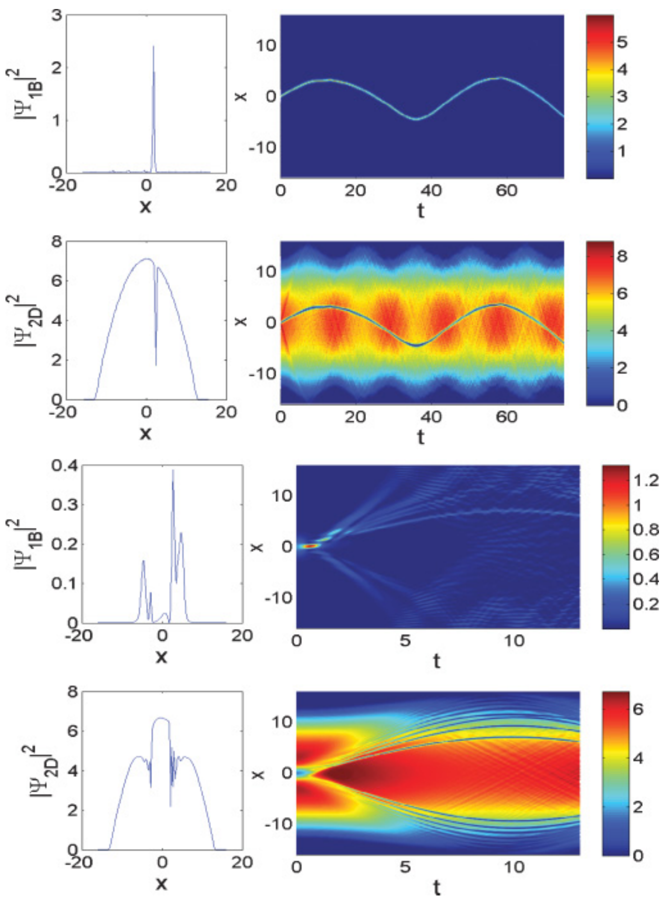

FIG. 2. (Color online) Evolution of a bright-dark soliton pair in a two-component BEC composed of ^{23}Na and ^{87}Rb atoms. Intraspecies scattering length $a_{12} = 6.831$ nm ($b_{12} = 7.25$) satisfies Eq. (1) (top two panels), while $a_{12} = 3.769$ nm ($b_{12} = 4$) deviates from Eq. (1) (bottom two panels). Other parameters are $a_{11} = 2.7$ nm ($b_{11} = 3.4$), $a_{22} = 5.5$ nm ($b_{22} = 3.6$), $m_1 = 23$ a.u., $m_2 = 87$ a.u., $\omega_{1,\perp} = 2\pi \times 710$ Hz, $\lambda_1 = \lambda_2 = 0.25$, $v = 0.15$, $N_1 = 500$, and $N_2 = 58\,000$. The snapshots are taken at $t = 20$, and $t = 2$, respectively. The distance x and time t are measured in units of $a_\perp = 786.7$ nm and $\tau = 0.22$ ms.

movement of the solitons, the dark component still captures the bright soliton during the motion.

In Fig. 2 the evolution of a bright-dark soliton pair in a binary BEC composed of ^{23}Na and ^{87}Rb atoms is plotted with corresponding snapshots of the density distribution. The upper two panels exhibit the bright (^{23}Na) and dark (^{87}Rb) excitations, respectively, which are stable for a long period due to the fine tuning of scattering lengths a_{ij} $(i,j = 1,2)$ which satisfy the P test Eq. (1). On the lower two panels of Fig. 2 we see, however, that the initial soliton excitations do not remain stable but are rapidly dissolved due to detuning the interspecies scattering length a_{12} from the value obeying the integrability condition expressed by Eq. (1).

In summary, both examples exhibited in Figs. 1 and 2 show that a long-lived stability of the bright-dark soliton pairs can be achieved only if the interatomic interaction parameter a_{12} (or b_{12}) is chosen according to Eq. (1). This observation emphasizes that there may be situations in the creation of two-component BECs when fine tuning of scattering lengths according to the P-test formula Eq. (1) may prove useful.

At the end of this section we briefly mention an early investigation of the stability of a heterogeneous two-component Bose-Einstein condensate by Law *et al.* [37]. In this work a linear stability analysis was carried out by calculating the lowest eigenvalue of an excitation. In this approach the appearance of a negative eigenvalue signals instability. It was shown for a sodium-rubidium system, as discussed here, that stability occurs only in the finite range of the interspecies scattering length. The direct quantitative comparison with our work, however, is less straightforward because Law *et al.* assumed a spherically symmetric condensate, while we analyze a quasi-one-dimensional model.

B. Static bright-bright soliton pairs

Let us now investigate the temporal stability of a static ($v = 0$) bright-bright soliton pair obtained as the exact solution of Eqs. (5a) and (5b) in the absence of a trapping potential ($\lambda_i = 0$). The solutions have the form of Eq. (11), where $\varphi_i(x)$ are chosen to have the functional forms given in Eqs. (18a) and (18b).

The existence conditions Eq. (19) prescribe the relations between domains of the inter- and intraspecies coupling strengths b_{ij}, which are listed in Table II. Moreover, the common wave vector is $k = 1/(2C_1)$.

Scenario 4, for example, describes two condensates for which the intraspecies interactions are repulsive. This situation, using a Hartree-Fock calculation, was theoretically analyzed [38] soon after the observation of overlapping condensates prepared from two hyperfine states of ^{87}Rb [2]. For this case, i.e., $m_1 = m_2$, it was established that the two condensates cannot coexist if $|a_{12}| < \sqrt{a_{11}a_{22}}$. Our approach reproduces and extends this result for the case of different species. This surprisingly simple relation can be understood using energetic arguments; if b_{12} overcomes the geometric mean of the intraspecies interaction strengths, the repulsion between the two condensates will separate the two condensates completely and they will no longer overlap. However, if the two species attract each other enough, i.e. $b_{12} < -\sqrt{b_{11}b_{22}}$, the attraction will dominate and can counteract the individual repulsion present in each component.

Another interesting scenario here is the one listed under case 3a in Table II, showing that it is possible to create a bright-bright pair within the range $0 < b_{12} < \sqrt{b_{11}b_{22}}$, in spite of the repulsive interatomic interaction. In order to investigate the stability of the bright-bright soliton pair in this domain we simulate the temporal evolution of the BEC system

TABLE II. Various domains of inter- and intraatomic interaction strengths b_{ij} permitting the existence of a bright-bright soliton pair.

Case	b_{11}	b_{22}	Constraint on b_{12}		
1	+	−	$b_{12} < b_{22}/\kappa$		
2	−	+	$b_{12} < b_{11}\kappa$		
3a	−	−	$b_{22}/\kappa < b_{12} < \sqrt{b_{11}b_{22}}$	if	$\kappa^2 b_{11} < b_{22}$
3b			$b_{12} < b_{11}\kappa$	if	$\kappa^2 b_{11} < b_{22}$
3c			$b_{11}\kappa < b_{12} < \sqrt{b_{11}b_{22}}$	if	$\kappa^2 b_{11} > b_{22}$
3d			$b_{12} < b_{22}/\kappa$	if	$\kappa^2 b_{11} > b_{22}$
4	+	+	$b_{12} < -\sqrt{b_{11}b_{22}}$		

composed of ^{7}Li and ^{39}K atoms accessible for experiments. As Fig. 3 shows, depending on the value of the interspecies interaction, two types of instability may occur. At values of a_{12} less than a critical value of about 0.275 nm, the two standing solitons begin to repel each other (first two panels) and depart from each other as though they were particles, preserving the total zero momentum. Above the critical a_{12} value the soliton with constituents of the smaller mass splits into two equal parts and the heavier component becomes a breather, keeping its original place (third pair of panels). At the critical value of a_{12} both types of instability can be observed (third and fourth panel) simultaneously.

Similar instability effects of bright-bright and other soliton pairs have also been observed [39]. The instability is explained by Kevrekidis *et al.* [40] as the appearance of a negative eigenvalue pair obtained by a linear stability analysis. It has also been shown that higher-order bright-bright soliton pairs would exhibit instability irrespective of the system parameters. Interestingly, it is possible for one of the higher-order bright solitons, i.e., the one that has the stronger self-attraction, to recover its stability by collapsing into one bright soliton and expelling the other component from its original position.

Finally, it is important to note here that the phases of the divided solitons are equal; therefore, these particle-like wave packets remain coherent with each other. Similarly to an optical beam splitter where light is divided into two coherent beams, one could divide these matter waves and use one of them as a probe and the other one as a control packet. The probe packet could undergo transformations, while the control packet is left to evolve freely, thereby allowing a phase difference to build up between the two packets. If the two packets are brought together again, the phase difference could cause an interference pattern that allows one to quantify coherence. This may potentially be helpful for calibration purposes as well.

C. Dark-dark soliton pairs

Finally, we examine the third possible combination of soliton pairs—a dark soliton being excited in each condensate. Interestingly this pairing can be stable even if the interaction inside each condensate is attractive (a_{11}, $a_{22} < 0$). The dark-dark solitons are described by the following formulas:

$$\widetilde{\psi}_1^{\mathrm{DD}} = \left[i\sqrt{-C_1}\,v + \Phi_1^{\mathrm{TF}}(0)\varphi_1^{\mathrm{DD}}(x - vt)\right] \exp\left(-i\widetilde{E}_1^{\mathrm{DD}}t\right) \times \exp\left[-i\left(\frac{b_{12}C_2}{\kappa^2} - b_{11}C_1\right)v^2 t\right], \quad (23a)$$

$$\widetilde{\psi}_2^{\mathrm{DD}} = \left[i\frac{\sqrt{C_2}}{\kappa}\,v + \Phi_2^{\mathrm{TF}}(0)\varphi_2^{\mathrm{DD}}(x - vt)\right] \exp\left(-i\widetilde{E}_2^{\mathrm{DD}}t\right) \times \exp\left[-i\left(\frac{b_{22}C_2}{\kappa^2} - b_{12}C_1\right)v^2 t\right]. \quad (23b)$$

For our numerical investigations a ^{87}Rb–^{87}Rb system has been chosen, with repulsive intraspecies interactions, $a_{11} = 5.335$ nm and $a_{22} = 5.665$ nm taken from Ref. [41]. This choice of coupling corresponds to scenario 4 of Table III. Tuning a_{12} into the positive regime results in stable dark-dark soliton pairs (see top two panels of Fig. 4). In the bright-bright case we have found that if the intraspecies interactions are attractive and the interspecies interactions are repulsive,

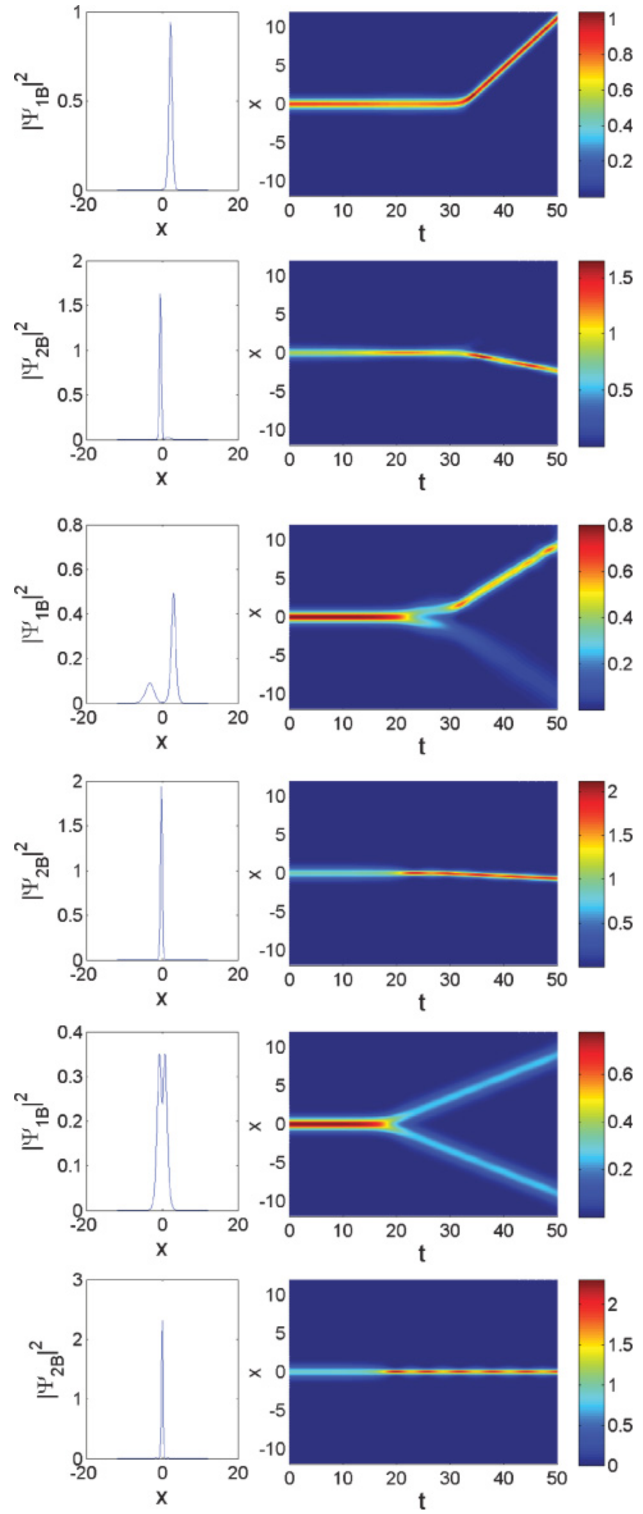

FIG. 3. (Color online) Evolution of a bright-bright soliton pair in a binary BEC composed of ^{7}Li and ^{39}K atoms. Intraspecies scattering lengths and atom numbers are $a_{12} = 0.2$ nm ($b_{12} = 0.46$), $N_2 = 2029$ (first two panels), $a_{12} = 0.275$ nm ($b_{12} = 0.64$), $N_2 = 2270$ (second pair of panels), and $a_{12} = 0.3$ nm ($b_{12} = 0.7$), $N_2 = 2347$ (third pair of panels). Other parameters are $a_{11} = -1.4$ nm ($b_{11} = -3.93$), $a_{22} = -0.9$ nm ($b_{22} = -1.07$), $m_1 = 7$ a.u., $m_2 = 39$ a.u., $\omega_{1,\perp} = 2\pi \times 710$ Hz, $\lambda_1 = \lambda_2 = 0$, $v = 0$, and $N_1 = 2000$. The snapshots are taken at $t = 35$, $t = 35$, and $t = 20$, respectively. The distance x and time t are measured in units of $a_\perp = 1426$ nm and $\tau = 0.22$ ms.

TABLE III. Various domains of inter- and intraatomic interaction strengths b_{ij} permitting the existence of a dark-dark soliton pair.

Case	b_{11}	b_{22}	Constraint on b_{12}		
1	+	−	$b_{12} > b_{11}\kappa$		
2	−	+	$b_{12} > b_{22}/\kappa$		
3	−	−	$b_{12} > \sqrt{b_{11}b_{22}}$		
4a	+	+	$-\sqrt{b_{11}b_{22}} < b_{12} < b_{22}/\kappa$	if	$\kappa^2 b_{11} > b_{22}$
4b			$b_{12} > b_{11}\kappa$	if	$\kappa^2 b_{11} > b_{22}$
4c			$-\sqrt{b_{11}b_{22}} < b_{12} < b_{11}\kappa$	if	$\kappa^2 b_{11} < b_{22}$
4d			$b_{12} > b_{22}/\kappa$	if	$\kappa^2 b_{11} < b_{22}$

the solutions are unstable. We have tested numerically that this observation is valid in the dark-dark case as well, if the sign of the interactions is inverted. Furthermore, our numerical calculation provided an interesting phenomenon in the dynamics of these solitons. Preparing the dark solitons in the same way as before (i.e., by superimposing onto the ground state) but reversing the sign of a_{12} resulted not only in losing the long-term stability but also in the decay of a dark soliton in one of the components and the emergence of a secondary dark soliton in the other component (bottom two panels of Fig. 4).

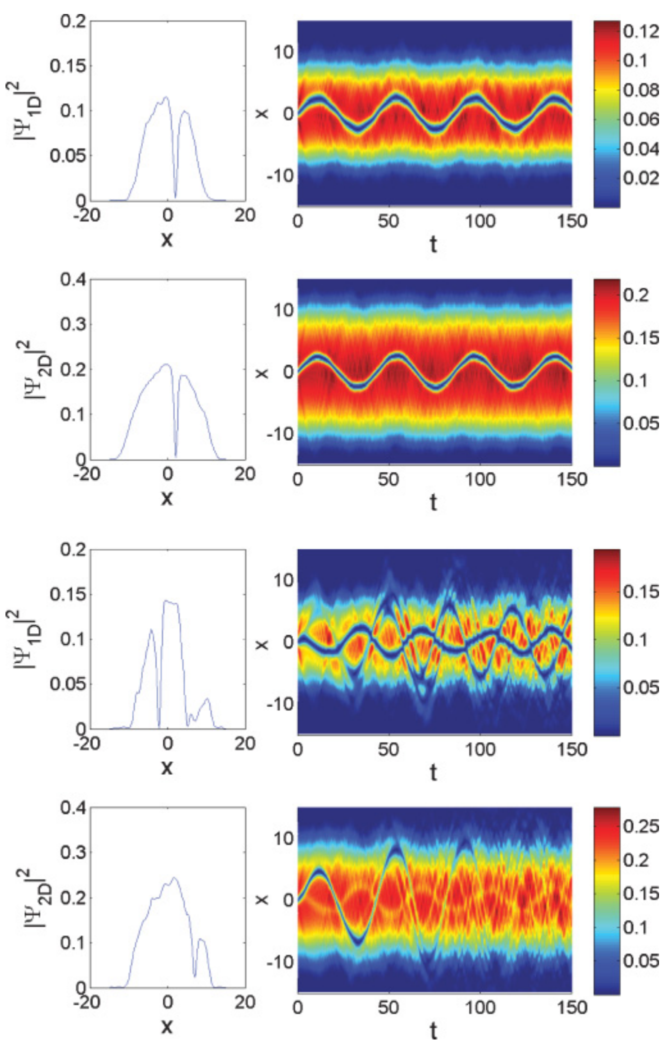

FIG. 4. (Color online) Evolution of a dark-dark soliton pair in a binary BEC composed of ^{87}Rb and ^{87}Rb atoms. Intraspecies scattering lengths are $a_{12} = 1.5$ nm ($b_{12} = 3.62$) (top panel) and $a_{12} = -1.5$ nm ($b_{12} = -3.62$) (bottom panel). Other parameters are $a_{11} = 0.97 \times 5.5$ nm ($b_{11} = 13.04$), $a_{22} = 1.03 \times 5.5$ nm ($b_{22} = 13.52$), $m_1 = 87$ a.u., $m_2 = 87$ a.u., $\omega_{1,\perp} = 2\pi \times 710$ Hz, $\lambda_1 = \lambda_2 = 0.2$, $v = 0.2$, $N_1 = 500$, and $N_2 = 1600$. The snapshots are taken at $t = 50$. The distance x and time t are measured in units of $a_\perp = 404.5$ nm and $\tau = 0.22$ ms.

IV. SUMMARY

We have considered the existence and stability of soliton excitations in a two-component Bose-Einstein condensate both analytically and numerically. Our model allows the components to represent different elements ($m_1 \neq m_2$), but we also include those cases when two hyperfine states of the same element constitute the condensates. We exclude the possibility that these components can transmute into each other; i.e., the hyperfine states cannot be driven into each other. The dynamics of these condensates, within the mean-field zero-temperature approximation, are governed by the coupled Gross-Pitaevskii equations. We have chosen to make our presentation suitable for combining analytical results with earlier numerical investigations, e.g., Refs. [26,32], and [42].

The occurrence of particle-like excitations together with conserved quantities is associated with the integrability of a nonlinear evolution field equation, such as the coupled Gross-Pitaevskii equations. Using the results of a recent Painlevé analysis of the coupled Gross-Pitaevskii equation [26], we have shown how the system parameters determine the integrability of this system. However, for the CGP equations the studies so far have been restricted to either equal coupling coefficients ($b_{11} = b_{12} = b_{22}$) and/or equal masses. We note here that excitations with long lifetimes may exist for a nonlinear evolution equation even when the integrability conditions are violated [43], but these cases are possibly exceptional and do not represent the generic behavior.

We have examined those ranges of system parameters that permit coupled soliton solutions of the governing equations (5a) and (5b). Here, we have utilized the two well-known one-soliton solutions of the one-component nonlinear Schrödinger equation: the bright and dark solitons. These excitations then spatially modify the Thomas-Fermi ground state in our theoretical description or the appropriate ground state in our numerical simulation. We have found analytically that each possible pair of these solitons has a range of system parameters where they are stable, and we have presented these ranges in Tables I, II, and III. One can present these findings differently if the intraspecies coupling coefficients are held relatively fixed and only the interspecies one is tuned. For example, if we assume b_{11} and b_{22} to be positive (effective repulsive interaction) then Tables I, II, and III can be combined into one graph (see Fig. 5).

Moreover, we have also examined how the stability of these soliton pairs changes if the interspecies coupling coefficient is detuned from the value predicted by the Painlevé analysis via Eq. (1). It has been shown, irrespective of the pairing, that the stability is lost, although the pairs were not equally sensitive to the detuning, e.g., the motion of the bright-dark pair became erratic and preserved its periodicity only qualitatively after changing a_{12} from 5.5 to 5.4 nm.

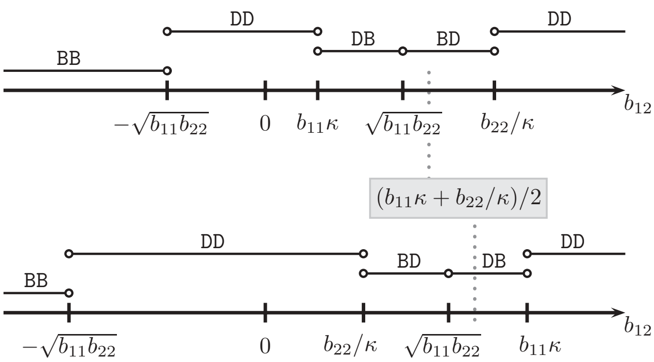

FIG. 5. Ranges of the interspecies coupling coefficient b_{12} in which different types of soliton pairs can exist and are stable. The top graph is valid if $\kappa^2 b_{11} < b_{22}$, while the lower graph is for the complementary case, i.e., $\kappa^2 b_{11} > b_{22}$. The dotted line shows the result of the Painlevé test Eq. (1) in the case of harmonic trapping potentials.

Two types of instability of static bright-bright soliton pairs composed of species with unequal masses have been observed. When the interspecies interaction lies below a critical value ($0 < b_{12} < b_{12}^{\mathrm{cr}}$), the static bright-bright pair evolves into a repulsive, momentum-conserving, moving soliton pair. When $b_{12} > b_{12}^{\mathrm{cr}}$, then one bright soliton (the constituent with smaller mass) splits into two equal portions of the same phase while the other bright soliton becomes a breather.

Well below the critical temperature of the Bose-Einstein condensate, we expect our description to be adequate, and the results could help experimentalists to modify the scattering lengths via the Feshbach resonance into a range where stable soliton pairs exist. As the temperature increases, however, the interaction with the thermal cloud becomes more and more important and can no longer be neglected. We have not yet examined how the interplay between the condensates and the thermal clouds (for each component) would modify the dynamics. This needs further research beyond the mean-field description.

ACKNOWLEDGMENTS

D. Schumayer acknowledges financial support from NERF-UOOX0703 (NZ) and also from the University of Otago. G. Csire and B. Apagyi thank DFG for subsidizing their stay at the Institute of Theoretical Physics, University of Giessen.

[1] I. Bloch, J. Dalibard, and W. Zwerger, Rev. Mod. Phys. **80**, 885 (2008).
[2] C. J. Myatt, E. A. Burt, R. W. Ghrist, E. A. Cornell, and C. E. Wieman, Phys. Rev. Lett. **78**, 586 (1997).
[3] D. M. Stamper-Kurn, M. R. Andrews, A. P. Chikkatur, S. Inouye, H.-J. Miesner, J. Stenger, and W. Ketterle, Phys. Rev. Lett. **80**, 2027 (1998).
[4] G. Modugno, G. Ferrari, G. Roati, R. J. Brecha, A. Simoni, and M. Inguscio, Science **294**, 1320 (2001).
[5] G. Thalhammer, G. Barontini, L. De Sarlo, J. Catani, F. Minardi, and M. Inguscio, Phys. Rev. Lett. **100**, 210402 (2008).
[6] M. Mudrich, S. Kraft, K. Singer, R. Grimm, A. Mosk, and M. Weidemüller, Phys. Rev. Lett. **88**, 253001 (2002).
[7] K. Pilch, A. D. Lange, A. Prantner, G. Kerner, F. Ferlaino, H.-C. Nägerl, and R. Grimm, Phys. Rev. A **79**, 042718 (2009).
[8] S. B. Papp, J. M. Pino, and C. E. Wieman, Phys. Rev. Lett. **101**, 040402 (2008).
[9] D. Schumayer and B. Apagyi, Phys. Rev. A **65**, 053614 (2002).
[10] A. Hasegawa and M. Matsumoto, *Optical Solitons in Fibers*, 3rd ed. (Springer-Verlag, Berlin, 2003).
[11] S. Burger, K. Bongs, S. Dettmer, W. Ertmer, K. Sengstock, A. Sanpera, G. V. Shlyapnikov, and M. Lewenstein, Phys. Rev. Lett. **83**, 5198 (1999).
[12] J. Denschlag *et al.*, Science **287**, 97 (2000).
[13] L. Khaykovich, F. Schreck, G. Ferrari, T. Bourdel, J. Cubizolles, L. D. Carr, Y. Castin, and C. Salomon, Science **296**, 1290 (2002).
[14] K. E. Strecker, G. B. Partridge, A. G. Truscott, and R. G. Hulet, Nature (London) **417**, 150 (2002).
[15] P. Öhberg and L. Santos, Phys. Rev. Lett. **86**, 2918 (2001).
[16] J. Liu and Z. Hao, Phys. Rev. E **65**, 066601 (2002).
[17] T. Busch and J. R. Anglin, Phys. Rev. Lett. **87**, 010401 (2001).
[18] C. Becker, S. Stellmer, P. Soltan-Panahi, S. Dorscher, M. Baumert, E.-M. Richter, J. Kronjager, K. Bongs, and K. Sengstock, Nature Phys. **4**, 496 (2008).
[19] N. S. Ginsberg, J. Brand, and L. V. Hau, Phys. Rev. Lett. **94**, 040403 (2005).
[20] W.-H. Steeb, M. Kloke, and B.-M. Spieker, J. Phys. A **17**, L825 (1984).
[21] V. E. Zakharov, Zh. Eksp. Teor. Fiz. **62**, 1745 (1972) [Sov. Phys.-JETP **35**, 908 (1972)].
[22] V. E. Zakharov and S. V. Manakov, Theor. Math. Phys. **19**, 551 (1974).
[23] V. E. Zakharov and S. V. Manakov, Funct. Anal. Appl. **19**, 89 (1985).
[24] R. Sahadevan, K. M. Tamizhmani, and M. Lakshmanan, J. Phys. A **19**, 1783 (1986).
[25] P. A. Clarkson, Proc. R. Soc. Edinburgh **109A**, 109 (1988).
[26] D. Schumayer and B. Apagyi, J. Phys. A **34**, 4969 (2001).
[27] V. A. Brazhnyi, V. V. Konotop, V. M. Perez-Garcia, and H. Ott, Phys. Rev. Lett. **102**, 144101 (2009).
[28] S. Rajendran, P. Muruganandam, and M. Lakshmanan, J. Phys. B **42**, 145307 (2009).
[29] K. Nakkeeran, J. Phys. A **34**, 5111 (2001).
[30] E. Gross, Nuovo Cimento **20**, 454 (1961).
[31] L. P. Pitaevskii, Sov. Phys. JETP **13**, 451 (1961).
[32] X. Liu, H. Pu, B. Xiong, W. M. Liu, and J. Gong, Phys. Rev. A **79**, 013423 (2009).
[33] D. Schumayer and B. Apagyi, Phys. Rev. A **69**, 043620 (2004).
[34] J. Javanainen and J. Ruostekoski, J. Phys. A **39**, L179 (2006).

[35] L. Lehtovaara, J. Toivanen, and J. Eloranta, J. Comp. Phys. **221**, 148 (2007).

[36] T. Busch and J. R. Anglin, Phys. Rev. Lett. **84**, 2298 (2000).

[37] C. K. Law, H. Pu, N. P. Bigelow, and J. H. Eberly, Phys. Rev. Lett. **79**, 3105 (1997).

[38] B. D. Esry, C. H. Greene, J. J. P. Burke, and J. L. Bohn, Phys. Rev. Lett. **78**, 3594 (1997).

[39] J. Belmonte-Beitia, V. M. Perez-Garcia, and V. Brazhnyi, Commun. Nonlinear Sci. **16**, 158 (2011).

[40] P. G. Kevrekidis, H. Susanto, R. Carretero-González, B. A. Malomed, and D. J. Frantzeskakis, Phys. Rev. E **72**, 066604 (2005).

[41] D. S. Hall, M. R. Matthews, J. R. Ensher, C. E. Wieman, and E. A. Cornell, Phys. Rev. Lett. **81**, 1539 (1998).

[42] X.-X. Liu, X.-F. Zhang, and P. Zhang, Chin. Phys. Lett. **27**, 070306 (2010).

[43] D. Novoa, B. A. Malomed, H. Michinel, and V. M. Perez-Garcia, Phys. Rev. Lett. **101**, 144101 (2008).